

# High-Energy Excitations in Silicon Nanoparticles

Adam Gali,<sup>\*,†</sup> Márton Vörös,<sup>†</sup> Dario Rocca,<sup>‡</sup> Gergely T. Zimanyi,<sup>§</sup> and Giulia Galli<sup>‡</sup>

*Department of Atomic Physics, Budapest University of Technology and Economics, Budafoki út 8., H-1111, Budapest, Hungary, Chemistry Department, University of California, Davis, California 95616, and Physics Department, University of California, Davis, California 95616*

Received June 19, 2009; Revised Manuscript Received September 11, 2009

## ABSTRACT

We have investigated high energy excitations in  $\sim 1$ – $2$  nm Si nanoparticles (NPs) by ab initio time-dependent density functional calculations, focusing on the influence on excitation spectra, of surface reconstruction, surface passivation by alkyl groups, and the interaction between NPs. We have found that surface reconstruction may change excitation spectra dramatically at both low and high energies above the gap; absorption may be enhanced nonlinearly by the presence of alkyl groups, compared to that of unreconstructed, hydrogenated Si NPs, and by the interaction between NPs. Our findings can help interpret the recent experiments on multielectron generation in colloidal semiconductor NPs as well as help optimize photovoltaic applications of NPs.

Recently, effective multiexciton generation (MEG) was reported in several colloidal semiconductor nanoparticles (NPs).<sup>1</sup> In the initial step of the MEG process a high-energy incident photon generates a high-energy exciton when absorbed by a semiconductor. This exciton may decay through two main relaxation channels: either by emitting phonons or by creating other excitons. In bulk semiconductors the Coulomb interaction is strongly screened; thus the excitonic channel is suppressed. On the other hand, a high density of vibrational states is available for excitons to relax by emitting phonons. For these reasons, MEG is a 1% effect in excitonic relaxation in bulk semiconductors, and it is thus irrelevant for photovoltaic (PV) applications.

In contrast, in NPs quantum confinement effects reduce electronic screening, thus effectively enhancing Coulomb interactions, and vibrational density of states is reduced, with respect to the bulk, inducing a so-called “phonon bottleneck”.<sup>2</sup> These concomitant factors may help decrease the probability of excitons to decay through phonon emission and enhance the probability of excitonic relaxations, thus opening the way for multiexciton formation to become a dominant relaxation channel.

In MEG processes much of the incident photon energy is retained in electronic excitations; therefore proposals<sup>3,4</sup> to use of MEGs in NPs for efficient solar energy conversion raised high hopes. Highly efficient MEG was initially

reported in environmentally unfriendly II–VI compounds, e.g., PbSe and CdTe. However, recent studies on II–VI and III–V semiconductor nanoparticles found that MEG efficiencies are less pronounced than originally suggested.<sup>5–10</sup> It was also found that these efficiencies depend on the surface chemistry, the concentration of NPs in the solution, and even on extrinsic effects such as the stirring of the solution, related to possible charging of the NPs.<sup>11–13</sup>

Recently, MEG has also been reported for more environmentally friendly materials, such as Si. In particular, effective biexciton generation was found in colloidal silicon nanoparticles<sup>14</sup> and in Si NPs embedded in a SiO<sub>2</sub> matrix, where the size and the distance of Si NPs were both  $\sim 3$  nm.<sup>15</sup> In the latter case the photon absorbed by the NP is (partly) transferred to generate a distinct excited state within another, nearby Si NP. The energy transfer process is accompanied by the relaxation, in the NP where it originated, from a highly excited state toward the lowest-energy excited state.<sup>15</sup> For fabrication purposes, in PV applications all-solid embedded Si NP systems may be superior to colloidal architectures; however a strong dependence on the surface/interface structure may be present in both cases.

A poignant demonstration of the sensitivity of the photoluminescence (PL) spectrum to the presence of surface/interface defects has been recently presented for Si NPs embedded in SiO<sub>2</sub>.<sup>16</sup> The defects were originally identified by the features they induced in the spectrum. Then they were passivated by hydrogenation and subsequently reintroduced in the system by ultraviolet irradiation.<sup>16</sup> The corresponding features in the spectrum disappeared and reappeared accord-

\* Corresponding author, agali@eik.bme.hu.

<sup>†</sup> Department of Atomic Physics, Budapest University of Technology and Economics.

<sup>‡</sup> Chemistry Department, University of California, Davis.

<sup>§</sup> Physics Department, University of California, Davis.

ingly. In contrast, it has been shown that alkyl-functionalized colloidal Si NPs exhibit a PL spectrum which is insensitive to UV irradiation or water treatment.<sup>17,18</sup>

Remarkably, alkyl-functionalized Si NPs were found to exhibit an enhanced absorption, with respect to hydrogenated dots, suggesting an important role of the electronic surface states associated with alkyl groups. Moreover, Rosso-Vasic et al. fabricated silicon nanoparticles of diameter of about 1.5 nm and capped them with different alkyl groups in hexane solution.<sup>17</sup> These NPs exhibited significantly enhanced absorption and emission in solutions with higher concentration, and this was attributed to the electronic coupling between the NPs. A similar effect was also observed in previous MEG studies.<sup>11,17</sup>

On the theoretical side, three interesting proposals were put forward to explain MEG processes.<sup>19–21</sup> (i) the impact ionization (II) theory of Zunger et al.,<sup>20</sup> based on detailed pseudopotential and configurational interactions (CI) calculations, suggests that the Coulomb interaction between the exciton and multiexciton states is responsible for the efficient MEG. The work of ref 20 was followed by a theoretical screening of candidate materials<sup>22</sup> and by a detailed analysis specific to PbSe nanocrystals.<sup>23</sup> A full nonequilibrium description of the MEG process, emphasizing the important role of the density of states of the one-exciton states was given in ref 24.

(ii) The Klimov group developed the alternative scenario of “virtual exciton generation” (VEG).<sup>19</sup> In this picture the generation of the initial high-energy exciton takes place simultaneously and coherently with the generation of additional excitons.

(iii) Finally, Efros et al. suggested a third explanation.<sup>21</sup> In their coherent exciton states (CES) picture the incident photon generates a single exciton, which then coherently evolves into a multiexciton state, enabled by the degeneracy of these states.<sup>21</sup>

Noticeably, all these theoretical frameworks build on a detailed knowledge of single particle excitations; nevertheless most studies have so far focused on low lying excitations,<sup>25–30</sup> with very few studies exploring high-energy excitation spectra.<sup>20,22</sup> In addition, none of the existing calculations has used ab initio techniques and has investigated the role played by surface states.

In order to contribute to the understanding of the MEG process, we focus here on high-energy excitations in Si nanoparticles and we investigate the role of surface states, surfactants, and NP interactions on absorption processes. To this end, we have determined the excitation spectrum of Si NPs using time-dependent density functional theory at “low” energies:  $1E_g < E < 2E_g$ , and high energies:  $2E_g < E$ , where  $E_g$  is the optical gap.

We find that electronic surface states accompanying surface reconstruction may give rise to absorption processes substantially different from those of unreconstructed, hydrogenated Si NP, at both low and high energies. In addition, absorption is enhanced nonlinearly both by the presence of alkyl groups bound to the surface and by the interaction between Si NPs.

We carried out calculations with supercell geometries, plane wave basis sets, and pseudopotentials,<sup>31</sup> using the pwscf code. We used a 35 and 150 Ry cutoff for the wave function and charge density expansions, respectively. We checked the convergence of our results on representative Si NPs by increasing the cutoffs up to 60 and 300 Ry. The distance between the surface hydrogen atoms of the periodic images was larger than 0.7 nm. All geometries were fully relaxed. Absorption spectra were calculated using time-dependent density functional theory (TD-DFT), with the generalized gradient PBE functional in the exchange-correlation kernel<sup>32</sup> and the technique proposed in ref 33. For a relatively small cluster, TD-DFT may provide a qualitatively correct description of excitation processes (unlike for the case of bulk solids) and it is used here to discuss trends in excitation spectra of small Si dots, as a function of surface structure and composition. We consider NPs with 1.2 to 2 nm diameter ( $d$ ). While the optical gap at such small sizes is too big for direct PV applications, our results provide indications about the relative importance of surface states, passivants, and NP–NP interaction. In addition, our results can be directly compared to recent experiments on alkyl-capped Si NPs of similar sizes.<sup>17</sup>

We simulated Si NPs with different surface terminations. First we considered NPs where each surface dangling bond was terminated by a hydrogen atom (see Figure 3). This model may represent the “perfect”, unreconstructed Si NPs with no surface states. We then investigated the effect of surface reconstruction of hydrogenated Si NPs. Finally, we studied NPs terminated with alkyl groups, including hexyl and methyl groups present experimentally in hexane solvents. These molecules bind to the surface by forming Si–C bonds.

The interaction between the Si NPs was investigated by considering two different configurations in our supercell calculations: simple cubic and tetrahedral lattices of Si NPs (see Figure 3).

First we discuss the effect of the surface reconstruction on absorption spectra. In Si NPs, a  $2 \times 1$ -like reconstruction may take place on (100) facets. Figure 1 illustrates the spectrum for unreconstructed and reconstructed Si NPs with  $d = 1.2$  nm and  $d = 2$  nm diameters. Several features are apparent from this figure.

(i) The optical gap is substantially reduced by the surface reconstruction from 3.0 to 2.0 eV in  $d = 1.2$  nm Si NP. This is consistent with similar reductions reported in the literature, e.g., in refs 25 and 29. While the weight of the lowest energy peaks is visibly small in the reconstructed case, the absorption exceeds that of the nonreconstructed NP from about 2.7 eV onward, in the  $d = 1.2$  nm SiNP. The gap of nonreconstructed  $d = 2$  nm Si NP decreases to 2.0 eV, and the surface states appear as resonances below and close to the HOMO (highest occupied molecular orbital) and right above the LUMO (lowest unoccupied molecular orbital); these states give rise to peaks in the excitation spectrum of the reconstructed cluster, at about 2.2 and 2.4 eV, that are not present in the unreconstructed case. In other  $\sim 2$  nm reconstructed clusters,<sup>25</sup> the LUMO state has been found to be a surface state. It is therefore reasonable to expect that in

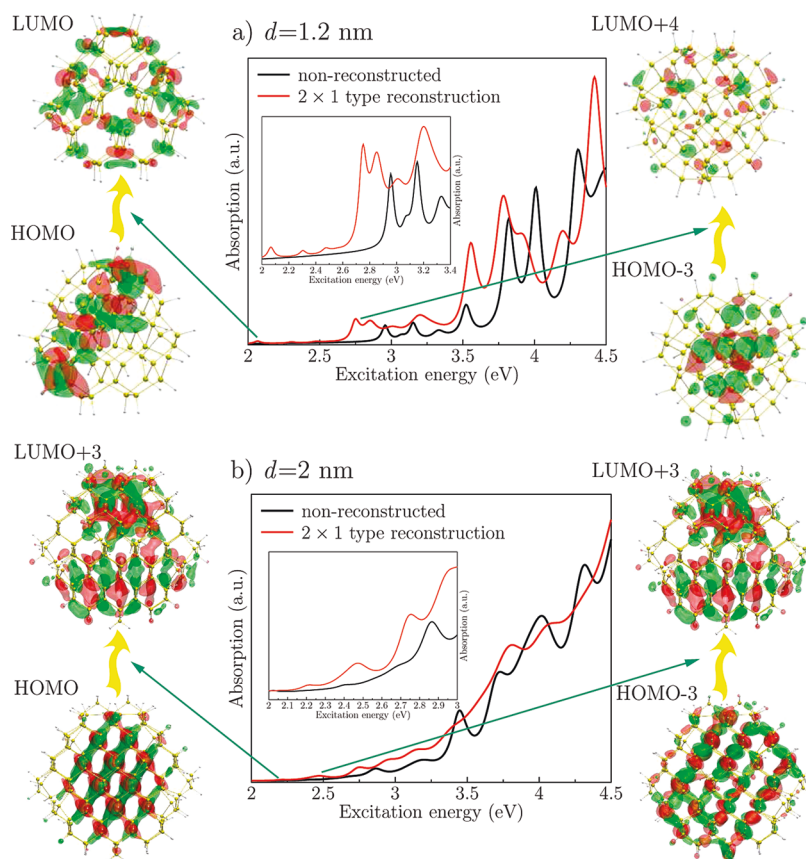


**Figure 1.** (a) The absorption spectra of reconstructed and nonreconstructed  $d = 1.2$  nm Si NPs. The peaks arising at low energy in the case of reconstructed surfaces and falling in the gap of the excitation spectrum of nonreconstructed ones are due to transitions between localized surface states. HOMO: highest occupied molecular orbital. LUMO: lowest unoccupied molecular orbital. The states on the right-hand side are indexed relative to the HOMO and LUMO states. The red/green lobes represent the isosurface of the positive/negative values of the corresponding square moduli of the wave function. (b) The absorption spectra of reconstructed and nonreconstructed  $d = 2$  nm Si NPs. The peaks just above the LUMO for the reconstructed Si NP are due to transitions between localized surface states.

reconstructed Si nanoparticles of about 2 nm, one finds surface states very close to the LUMO.

(ii) The absorption increases dramatically in the low-energy region of the reconstructed cluster. This is evident from the emergence of the pronounced new peaks both in the 2.7–3.0 eV range for  $d = 1.2$  nm Si NP and in the 2.2–2.4 eV range for  $d = 2$  nm Si NP, respectively, as well as the increase of the integrated spectral weight in the  $1E_g - 1.5E_g$  energy window.

(iii) The increase of the absorption of the reconstructed clusters (versus the nonreconstructed one) is *nonlinear*: the spectra integrated over higher energy windows increase more moderately than those obtained over the low energy window.

(iv) The presence of surface states gives rise to resonances at high energies.

The lowering of the gap induced by reconstruction and the substantial enhancement of the spectrum in the high-energy region suggest that surface reconstruction may help enhance MEG processes, whose onset is at  $2E_g$ , and maximum efficiency enhancement is obtained from the biexciton generation in the  $(2-3)E_g$  high energy range.

Importantly, we note that excitations in the low-energy region of  $(1-2)E_g$  also contribute to MEG process, as shown in ref 24, since the bi- and triexciton states are created from

all possible combinations of single excitonic states (subject to selection rules, of course). Therefore an increase in the low-energy density of excitations is a possible indication, although clearly rather indirect, of enhanced MEG efficiency.

We also note that surface states can act as traps for excited carriers with relatively long lifetime in small Si NPs. Hence they may be responsible for charging of NPs in transient absorption spectroscopy measurements and can lead to possible problems in interpretation of experiment.

We note that the increase of the effective Coulomb interaction in NP, compared to bulk, poses design challenges for their use in PV applications: while such an increase may enhance the efficiency of MEG, in principle it makes the extraction of the charge generated by MEG harder than in the bulk. However the presence of surface states, as predicted by our calculations, might help to make the charge extraction more effective.

We now turn our attention to the effect of the solvent on the spectrum of Si NPs. In the photoluminescence experiments on colloidal NPs, alkyl groups are often attached to the surface. To gauge an understanding of the effect of various passivants, we studied methyl ligands, the shortest alkyl group, and hexyl, the longest alkyl group considered in this work. We simulated a hierarchy of representative samples,

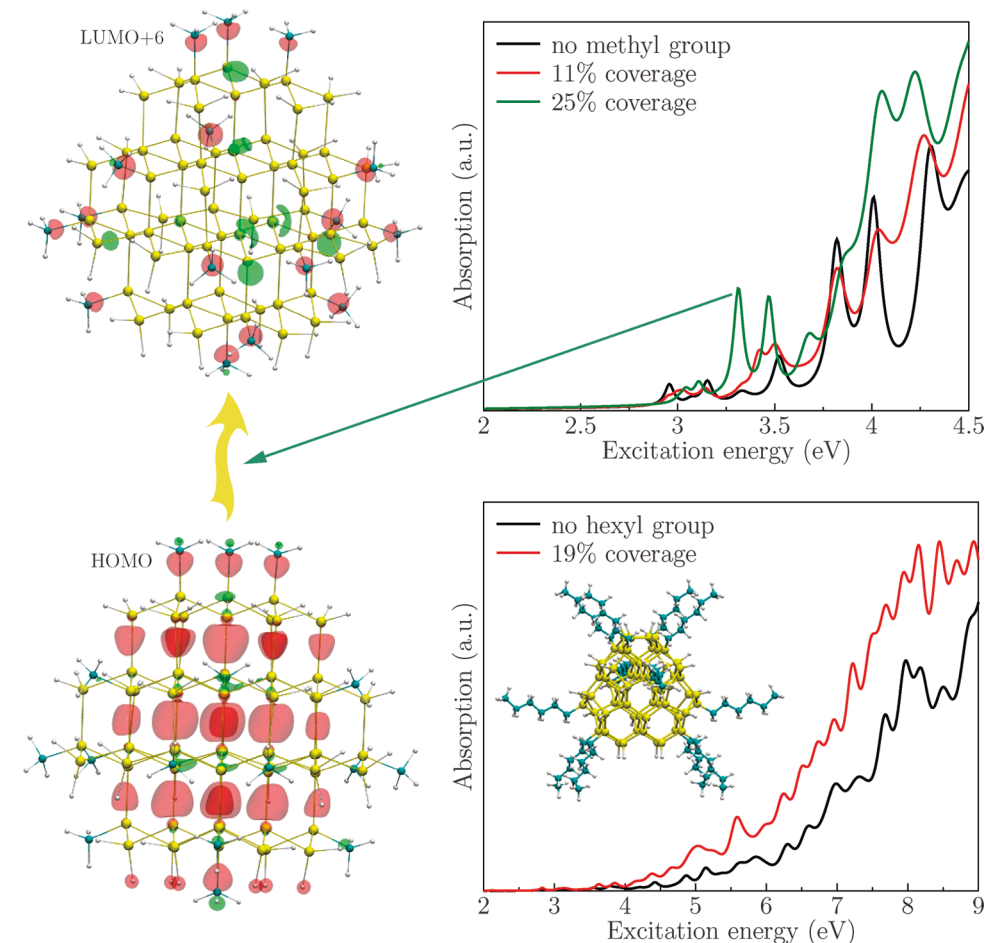


**Figure 2.** Excitation spectra of Si NPs terminated by methyl and hexyl groups compared to that of purely hydrogenated Si NPs. The peaks in the spectrum of alkyl-terminated dots can be attributed to the strong Si–C bonds present at the surface. The red/green lobes represent the isosurface of the positive/negative values of the square moduli of wave functions. HOMO: highest occupied molecular orbital. LUMO: lowest unoccupied molecular orbital. In the inset the configuration of 19% coverage with hexyl groups is shown.

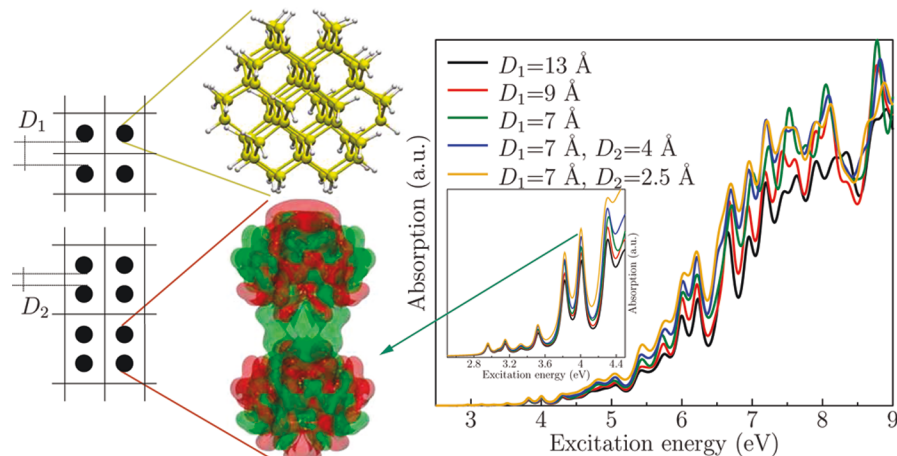
created by substituting H atoms at the surface by alkyl groups, with alkyl coverage varying from 1.5% to 25% (see Figure 2). Since the presence of long hexyl groups leads to very CPU intensive calculations, in this case we focused only on two coverages, 1.5% and 19%, and on 1.2 nm NPs. The hexyl groups were placed at the positions minimizing the repulsive interaction between the alkyl groups (see the inset in Figure 2).

Figure 2 shows the calculated spectra. Consistent with previous studies,<sup>26</sup> we found that the alkyl groups do not change the optical gap of the host Si NPs. At low surface coverages with methyl groups, the absorption spectrum does not change considerably relative to the one of purely hydrogen-terminated Si NPs. However, at higher coverages the spectrum exhibits new peaks above  $E_g$ . The new peaks correspond to transitions involving states localized on the surface Si–C bonds. The intensity of these peaks increases with increasing coverage by either the methyl or hexyl groups. We found that in the energy window from zero up to  $2E_g$  and up to  $3E_g$  the increase of absorption is around 45% and 10%, respectively, for methyl-terminated Si NPs (at 25% coverage), while it is more than 100% and more than 60% for hexyl-terminated Si NPs (at 19% coverage). The numbers associated here to spectral enhancement are

indicative of trends and not meant to be quantitative estimates for direct comparison with experiment. We also found that the enhancement of the spectrum is nonlinear and it is more pronounced in the case of a hexyl group, which might then be the most promising solvent for MEG processes.

The high sensitivity of the spectrum to the type of solvent may explain the recent observations that the MEG depends on the ligands attached to the NPs and on charging effects.<sup>11,13,34</sup>

In addition to various ligands, experimentally one may have different concentrations of NPs whose distance could be, in some cases, just a few angstroms (see refs 13 and 34). Such distances can be directly modeled in our calculations. As shown in Figure 3, in a simple cubic arrangement we calculated the spectrum for NP–NP distance ( $D_1$ ) varying from 0.7 to 1.3 nm along the three axes of the cell, while in the tetrahedral configuration the distance ( $D_2$ ) was varied between 0.25 and 0.4 nm with  $D_1 = 0.7$  nm. In the tetrahedral configuration two NPs were close to each other along one axis while they were  $D_1 = 0.7$  nm apart from each other along the remaining two axes. In both cases  $D_1$  and  $D_2$  were defined as the minimum distance between the hydrogen atoms bound to two neighboring NPs.



**Figure 3.** Excitation spectra of hydrogen-terminated  $d = 1.2$  nm Si nanoparticle with unreconstructed surfaces. Two different arrangements of SiNP within our supercell are shown schematically: (i) the simple cubic configuration where the distance between neighboring SiNPs is  $D_1$  in each direction, (ii) tetrahedral configuration where two neighboring SiNPs are closer to each other ( $D_2$ ) in one direction while the distance between their periodic images is  $D_1$  for all the other directions. The calculated absorption spectra are shown for different  $D_1$ ,  $D_2$  configurations. The tendency of increasing absorption for closer SiNPs is due to the interaction between delocalized empty states, as shown, e.g., in the figure for the  $D_1 = 7$  Å,  $D_2 = 2.5$  Å configuration. The red/green lobes represent the isosurface of the positive/negative values of  $4.5 \times 10^{-3}$  /bohr<sup>3</sup> of the square moduli of wave function. This state is mostly responsible for the peaks at around 4.0 eV as indicated by the arrow.

The calculated excitation spectrum for unreconstructed NPs is plotted in Figure 3 from  $E_g$  up to  $3E_g$ . Apparently, the onset of absorption starts at the same energy, about 2.9 eV. This energy is close to the experimental value ( $\sim 3.5$  eV) for Si NP with similar size.<sup>17</sup> The first peak originates from the HOMO  $\rightarrow$  LUMO transition. The position of HOMO and LUMO energies did not change as a function of the distance between the NPs.

At higher energies, however, the absorption clearly increases in all energy ranges as the NPs approach each other, and additional peaks can be detected. This can be qualitatively understood in terms of overlaps between single particle orbitals: As excitation energies are increased, states become more delocalized and hence the overlap between states belonging to neighboring NPs increases.

We integrated the intensity of absorption between  $E_g$  and  $2E_g$  and compared to that integrated intensity between  $2E_g$  and  $3E_g$  in order to estimate the enhancement of the absorption. By taking the two extreme cases of our samples, the cubic  $D_1 = 1.4$  nm and the tetrahedral  $D_2 = 0.25$  nm –  $D_1 = 0.7$  nm values, the enhancement is about twice as large between  $E_g$  and  $2E_g$  than between  $2E_g$  and  $3E_g$ . Our results show that *the NP–NP interactions increase the absorption profoundly*. Moreover, the enhancement is nonlinear as a function of excitation energy due to the interaction of the NPs. Therefore, in order to understand the high-energy phenomena such as the MEG, the NP–NP interaction needs to be taken account.

In summary, we have investigated high-energy excitations in silicon nanoparticles using TD-DFT. We found that surface reconstruction, surface termination with alkyl groups (mimicking possible solvent effects), and NP–NP interactions are all responsible for an enhancement of photon absorption, with respect to that found for isolated, hydrogen terminated, and unreconstructed clusters. The enhancements found in our

calculations depend nonlinearly on the energy: they are stronger in the  $1E_g - 2E_g$  low-energy region than in the  $2E_g - 3E_g$  high-energy region. Our findings provide indications how to enhance the efficiency of the MEG pathway for solar energy conversion. Encouragingly, the trends observed here are all consistent with those reported in recent experimental studies of colloidal NPs.

**Acknowledgment.** The authors gratefully acknowledge numerous useful discussions with V. Klimov, M. G. Bawendi, C. Delerue, and A. Zunger. A.G. acknowledges support from OTKA No. K-67886 and János Bolyai program from the Hungarian Academy of Sciences. D.R. and G.G. acknowledge support from Grants DOE-FG02-06ER46262 and NSF-CHE-0802907.

## References

- (1) Schaller, R. D.; Klimov, V. I. *Phys. Rev. Lett.* **2004**, *92*, 186601.
- (2) Bockelmann, U.; Bastard, G. *Phys. Rev. B: Condens. Matter Mater. Phys.* **1990**, *42*, 8947–8951.
- (3) Klimov, V. I. *J. Phys. Chem. B* **2006**, *110*, 16827–16845.
- (4) Nozik, A. J. *Chem. Phys. Lett.* **2008**, *457*, 3–11.
- (5) Nair, G.; Bawendi, M. G. *Phys. Rev. B: Condens. Matter Mater. Phys.* **2007**, *76*, 081304.
- (6) Pijpers, J. J. H.; Hendry, E.; Milder, M. T. W.; Fanciulli, R.; Savolainen, J.; Herek, J. L.; Vanmaekelbergh, D.; Ruhman, S.; Mocatta, D.; Oron, D.; Aharoni, A.; Banin, U.; Bonn, M. *J. Phys. Chem. C* **2008**, *112*, 4783–4784.
- (7) Ben-Lulu, M.; Mocatta, D.; Bonn, M.; Banin, U.; Ruhman, S. *Nano Lett.* **2008**, *8*, 1207–1211.
- (8) Trinh, M. T.; Houtepen, A. J.; Schins, J. M.; Hanrath, T.; Piris, J.; Knulst, W.; Goossens, A. P. L. M.; Siebbeles, L. D. A. *Nano Lett.* **2008**, *8*, 1713–1718.
- (9) Nair, G.; Geyer, S. M.; Chang, L.-Y.; Bawendi, M. G. *Phys. Rev. B: Condens. Matter Mater. Phys.* **2008**, *78*, 125325.
- (10) Ji, M.; Park, S.; Connor, S. T.; Mokari, T.; Cui, Y.; Gaffney, K. J. *Nano Lett.* **2009**, *9*, 1217–1222.
- (11) Luther, J. M.; Beard, M. C.; Song, Q.; Law, M.; Ellingson, R. J.; Nozik, A. J. *Nano Lett.* **2007**, *7*, 1779–1784.
- (12) McGuire, J. A.; Joo, J.; Pietryga, J. M.; Schaller, R. D.; Klimov, V. I. *Acc. Chem. Res.* **2008**, *41*, 1810–1819.
- (13) Beard, M. C.; Midgett, A. G.; Law, M.; Semonin, O. E.; Ellingson, R. J.; Nozik, A. J. *Nano Lett.* **2009**, *9*, 836–845.

- (14) Beard, M. C.; Knutsen, K. P.; Yu, P.; Luther, J. M.; Song, Q.; Metzger, W. K.; Ellingson, R. J.; Nozik, A. J. *Nano Lett.* **2007**, *7*, 2506–2512.
- (15) Timmerman, D.; Izeddin, I.; Stallinga, P.; Yassievich, I. N.; Gregorkiewicz, T. *Nat. Photonics* **2008**, *2*, 105.
- (16) Godefroo, S.; Hayne, M.; Jivanescu, M.; Stesmans, A.; Zacharias, M.; Lebedev, O. I.; Tendeloo, G. V.; Moshchalkov, V. V. *Nat. Nanotechnol.* **2008**, *3*, 174–178.
- (17) Rosso-Vasic, M.; Spruijt, E.; van Lagen, B.; Cola, L. D.; Zuilhof, H. *Small* **2008**, *4*, 1835–1841.
- (18) Gupta, A.; Swihart, M. T.; Wiggers, H. *Adv. Funct. Mater.* **2009**, *19*, 696–703.
- (19) Schaller, R.; Agranovich, V.; Klimov, V. *Nat. Phys.* **2005**, *1*, 189.
- (20) Franceschetti, A.; Anh, J.; Zunger, A. *Nano Lett.* **2006**, *6*, 2191.
- (21) Shabaev, A.; Efros, A.; Nozik, A. *Nano Lett.* **2006**, *6*, 2856.
- (22) Luo, J.-W.; Franceschetti, A.; Zunger, A. *Nano Lett.* **2008**, *8*, 3174–3181.
- (23) Franceschetti, A. *Phys. Rev. B* **2008**, *78*, 075418.
- (24) Allan, G.; Delerue, C. *Phys. Rev. B: Condens. Matter Mater. Phys.* **2008**, *77*, 125340.
- (25) Puzder, A.; Williamson, A. J.; Reboredo, F. A.; Galli, G. *Phys. Rev. Lett.* **2003**, *91*, 157405.
- (26) Reboredo, F. A.; Galli, G. *J. Phys. Chem. B* **2005**, *109*, 1072–1078.
- (27) Tiago, M. L.; Chelikowsky, J. R. *Phys. Rev. B: Condens. Matter Mater. Phys.* **2006**, *73*, 205334.
- (28) Zhou, Y.; Saad, Y.; Tiago, M. L.; Chelikowsky, J. R. *Phys. Rev. E: Stat., Nonlinear, Soft Matter Phys.* **2006**, *74*, 066704.
- (29) Wang, X.; Zhang, R. Q.; Lee, S. T.; Frauenheim, T.; Niehaus, T. A. *Appl. Phys. Lett.* **2008**, *93*, 243120.
- (30) König, D.; Rudd, J.; Green, M. A.; Conibeer, G. *Phys. Rev. B: Condens. Matter Mater. Phys.* **2008**, *78*, 035339.
- (31) Vanderbilt, D. *Phys. Rev. B: Condens. Matter Mater. Phys.* **1990**, *41*, 7892–7895.
- (32) Perdew, J. P.; Burke, K.; Ernzerhof, M. *Phys. Rev. Lett.* **1996**, *77*, 3865–3868.
- (33) Rocca, D.; Gebauer, R.; Saad, Y.; Baroni, S. *J. Chem. Phys.* **2008**, *128*, 154105.
- (34) Koleilat, G. I.; Levina, L.; Shukla, H.; Myrskog, S. H.; Hinds, S.; Pattantyus-Abraham, A. G.; Sargent, E. H. *ACS Nano* **2008**, *2*, 833–840.

NL901970U